RSC Advances

PAPER

Cite this: *RSC Adv.*, 2016, **6**, 72080

Spotlight on ultrasonic fracture behaviour of nanowires: their size-dependent effect and prospect for controllable functional modification†

H. Dai, T. Y. Wang and M. C. Li*

Received 5th June 2016
Accepted 24th July 2016

DOI: 10.1039/c6ra14559k

www.rsc.org/advances

Ultrasonic deformation and even fracture of one-dimensional nanomaterials usually occur under sonication, which is likely to have a significant effect on their physical and chemical properties. However, this process and the mechanism underlain are still unknown and yet to be found out. Herein, we establish a 'bubble-jet impact' model to study the specific behaviour of fracture evolution of nanowires in sonication processing. By recording the plastic deformation and absorbency of certain sonicated nanowires, *e.g.*, Ag and Cu, a strong size-dependent breakage induced by the bubble-jet is well validated, which shows that relatively long nanowires tend to fracture by bending while short or medium-length nanowires, as fractured remainders of long ones, have the inclination to be tensile broken. The transition point between the two types of fractures has also been discovered. Our results not only provide guidelines for ultrasonic dispersion, but also pioneer a possible way for controllable functional modification of one-dimensional nanomaterials.

Introduction

Ultrasonic treatment is widely used for surface cleaning, since it is not an exotic process, and is easy to implement with a bulk reactor near room temperature. The effects of sonication are derived primarily from cavitation, where liquids rupture and form vapor bubbles when the liquid pressure is decreased below a critical tension. Then, the bubble collapse results in an enormous concentration of kinetic energy of liquid motion. The collapse creates local extreme pressures and shock waves, and then ultrasonic cavitation occurs when the threshold energy density is exceeded by an acoustic compression wave. Recent experiments and theories have shown the extreme conditions reached during cavitation: in the collapsed cavities, liquid motion rates up to 10^9 s^{-1}.[1,2] Under the routine sonication condition, commonly with a frequency of 20 kHz, cavitation-induced bubble contraction leads to bubble jet and shock waves that exist simultaneously. When materials are being sonicated, except for the effect of cleaning and dispersion, unwanted deformation, corrosion or even breakage of the materials suspended in the liquid occur even for a short sonication time.[3–6] Thus, ultrasonic fragmentation and the structure modifications induced by the bubble collapse have become the latest research hotspots for ultrasonic technologies.

State Key Laboratory of Alternate Electrical Power System with Renewable Energy Sources, School of Renewable Energy, North China Electric Power University, Beijing 102206, China. E-mail: mcli@ncepu.edu.cn

† Electronic supplementary information (ESI) available. See DOI: 10.1039/c6ra14559k

Significant sonication-induced changes of materials are driving the exploration of the mechanism behind the ultrasonic fragmentation to suspended materials in chemically inert media.[7–12] For fixed solid–liquid interfaces, only those bubbles within a distance from the solid equal to the bubble radius can produce any damage on solid surface by shock waves, which has been concluded by F. G. Hammitt *et al.*[13] Also, it has been found that the selective corrosion on the solid surface is mainly caused by the bubble jet impactions.[14] It can be seen that the ultrasonic breakages of the fixed solid–liquid interfaces are being researched upon a lot and the damage mechanisms coincide well with the experiment results. These works are taken as the theoretical basis of ultrasonic fragmentation mechanism.

Nanomaterials whose properties are much more dependent on their morphologies have aroused explosive growth in research.[15–17] Generally, nanomaterials are prone to reunite, entanglement or even agglomeration and become problematic for use in micro-electronics and photonics device fabrication.[18–20] Routine treatment for dispersion of these nanomaterials is usually done by the sonication.[21] For nanomaterials at the unfixed solid–liquid interface condition (suspended in the liquid), the ultrasonic damage mechanisms are considered different from the fixed solid–liquid interfaces.[22] Recently, by successfully predicting the ultimate lengths of sonicated nanowires, Y. Y. Huang *et al.* found that the effects of tensile break of one-dimensional nanomaterials suspended in solution resulted from bubble contraction which shows significant improvements in the measurements of the mechanical properties of nanostructures.[22,23] However, in their work, the effects of tensile break failed to explain the common bending

phenomenon. Due to the morphology-dependent properties of nanomaterials, it is necessary to find out sonication effects on the fragmentation of nanomaterials in the unfixed solid–liquid interface condition.

Herein, a 'bubble-jet impacted' model has been established to study the behavior of ultrasonic fragmentation evolution of one-dimensional nanomaterials (nanowires) in the unfixed solid–liquid interface condition. By recording the plastic deformation and absorbency of certain sonicated nanowires, *e.g.*, Ag and Cu, a size-dependent breakage rule is well validated, which shows that relatively long nanowires tend to fracture by bending fragmentation mechanism, while short or medium-length nanowires, including the fractured remnants of long ones, can easily undergo the tensile fragmentation. The transition points between the two types of fragmentations have also been provided. Our results provide excellent explanations for the common bending phenomenon and breakage rates of nanowires under sonication. Furthermore, the discovery of the transition points provides guidelines for nanomaterial ultrasonic dispersion and functional modification of one-dimensional nanomaterials.

Experiments

Ag nanowires (with average diameter of 140 nm and length of 26 μm) and Cu nanowires (with average diameter of 130 nm and length of 8 μm) were purchased from Nanjing XFNANO Materials Tech Co., Ltd. Both of the metal nanowires were dispersed in ethanol solution (about 0.2 wt%) and sonicated (20 kHz, 15 W cm^{-2}) at 0 °C in ice bath to avoid heating up, respectively. Absolute ethanol (99.9%) and n-type Si (100) substrates with single side polished surface for well separation of metal nanowires were used in our study. After sonication, spreading method was utilized to separate the nanowires on the surfaces of Si substrates.

The morphology and lattice of Ag nanowires were measured by optical microscopy (Yongxiang corp., Model 10XB-PC), field emission SEM (HITACHI UHR FE-SEM SU8010) and TEM (JEOL JEM 2100 LaB_6). Absorbance variations of Ag nanowires dispersion solution were measured by UV spectrophotometer (Hitachi S4800).

Results and discussion

In the sonication-induced fragmentation of nanowires, the previous recognition of the implosion dynamics of the cavitation bubble is based on an inward radial flow around a bubble. And the stress that is exerted on a suspended nanowire by the viscous forces is transmitted from the inward radial flow. Y. Y. Huang *et al.* set a model based on the inward radial flow around a bubble and successfully predicted the ultimate facture length of different types of nanowires. However, this simple model failed to explain the phenomena of serious bending deformation observed in sonication process. It should be noted that the velocity field of flow in ultrasonic process is very complex. A variety of experimental parameters, including ultrasound frequency, container geometry, acoustic power, and pulsing rates, determine the spatial distribution and frequency of bubble creation and implosion events. Under the routine sonication condition, the inward radial flow, bubble jet and shock waves can exist simultaneously. The latter two factors can also lead to high flow rate of the liquid and can also cause serious breakage on solid surface which were neglected in previous studies.[21,24] In general, suspended nanomaterials with multiple unfixed liquid/solid interfaces are able to provide ideal sites for sonication-generated cavitation bubbles and upon collapse, bubble jets with inclined direction from the liquid towards nanowires.[25] Thus, the possibility and detailed mechanism of the fragmentation behavior of suspended nanowires caused by bubble jet or shock waves should be clarified.

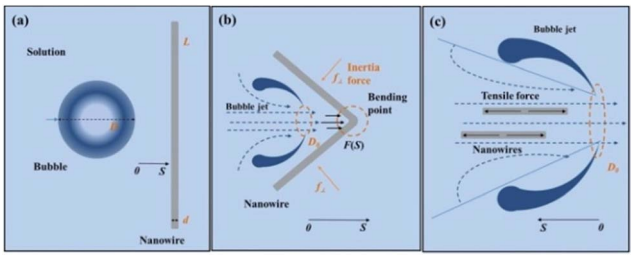

Fig. 1 Schematic diagram of different effects of bubble jet on varied-size nanowires (a) initial cavitation bubble induced by sonication in liquid solution; (b) bending fracture caused by the impact force; (c) tensile fracture caused by the tensile force.

We develop a 'bubble-jet impacted' model to describe the effect of bubble implosion dynamics on nanowires as shown in Fig. 1. The initial state of a cavitation bubble alongside a nanowire in liquid solution is provided as shown in Fig. 1(a), where D is the diameter of the bubble (about 10 μm), d denotes the diameter of the nanowire, L is its length and S is the distance between the nanowire and the bubble wall. Upon collapse as shown in Fig. 1(b), the vertical force F from bubble jet on the nanowire can be expressed as $F(S) = 0.5\rho a U(S)^2$. Where ρ represents the density of liquid (ethanol: 0.78×10^3 kg m^{-3}), a represents the effective action area of Ag nanowires (defined as $a = d \cdot D_0$, where D_0 denotes the diameter of the bubble jet, about 2–3 μm,[25] and is simplified to a constant here) and $U(S)$ represents the fluid velocity of the jet. In the free fluid field, the fluid velocity $U(S)$ of the jet can be expressed by $U(S)/U_0 = 0.96/(0.29 + 2\beta S/D_0)$, where U_0 is the initial velocity of the bubble jet, here set to 110 m s^{-1}, β is an empirical parameter, often chosen 0.7–0.8.[26] The stress σ of nanowire derived from F is thus:

$$\sigma = 8F(S)(L - D_0)/\pi d^3 \quad (1)$$

From eqn (1), we calculate the forces induced by the bubble jet on varied-size nanowires as shown in Fig. 2. The forces exerted on nanowires increases proportionally with length. In addition, the forces exert on nanowires with small d (diameter 100 nm) can reach up to several hundred GPa, which indicates that the forces induced by the bubble jet can cause damage on metal nanomaterials with the size in such range under this

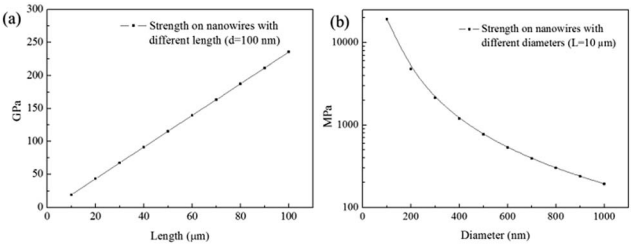

Fig. 2 Calculation results of the force induced by the bubble jet on varied-size nanowires (a) strength exert on nanowires (diameter: 100 nm) with lengths from 10 to 100 μm; (b) strength on nanowires (length: 10 μm) with diameters from 100 to 1000 nm.

sonication condition. Meanwhile, the forces exerted on nanowires (length of 10 μm) decrease sharply with the increase of d. When the nanowires diameters d increase to 1 μm, the forces exerted on nanowires decrease to only about one hundred MPa.

In order to clearly show the great power of the transited force $F(S)$, concrete values are set in eqn (1). There into, L is fixed to 25 μm and d to 100 nm, fitting the common property of metal nanowires. At $S = 0$, meaning the nanowire is almost touching the bubble, the resulting σ_{max} is approximately two orders larger than the strength σ_m of Ag or Cu nanowire (Ag: 174 MPa, Cu: 225 MPa).[23,27] With their distance increasing, $U(S)$ is attenuated in the free fluid field, but the bubble jet can still cause the fracture even when the nanowire is 30 μm away.

Since the value of σ reduces in linear proportion with L, indicating that the length of nanowires decreases, the force σ acting on them shows a sharp reduction. With L decreasing until approximating the value of D_0, the force σ approaches zero, meaning force on nanowires vanishes. Based on previous reports, the nanowires with such size can continue to break into shorter pieces in prolonged sonication. Consequently, there could be other fragmentation mechanisms here associated with the cavitation.

On the other hand, the nanowires can also be brought into the bubble interior by a tensile force originating from the bubble jet with the direction from point A to B as shown in Fig. 1(c). The bubble jet is shaped like a cone which satisfies the distribution as follows: $U(S)^* = U_0{D_0}^2/4(D_0 - \xi S)^2$, where ξ (estimated about 0.2–0.4) is derived from the ratio of D_0 to D. Referring to the deduction method,[18] the tensile force on nanowires due to the viscous drag of the bubble jet can be expressed as: $\sigma^* = 2d^{-2}\eta U_0{D_0}^2(D_0 - \xi S)^{-3}L^2$, where η is the viscosity of the fluid (0.01 Pa). The maximal stress σ^* acting on a nanowire is located at point O, and therefore we can describe the ultimate length as a function of tensile strengths as: $L_{lim} \approx 6.7 \times 10^{-4} d{\sigma_m}^{1/2}$. As expected, this predicted ultimate length is almost in accordance with the study by Huang *et al.*,[23] although different physics models are adopted. Hence, the further fracture of nanowires with length approximating to D_0 could be caused by the coactions of bubble contraction and bubble jet, when there is no effect of the impaction. Finally, a stable state of nanowires with ultimate length can be reached after long time sonication. It is found that the limiting length is only dependent on the diameter of the nanowires, and not affected by the other sonication parameters, including container geometry, power value and pulsing rate.

Based on the foregoing discussion, we therefore suggest that long nanowires ($L \gg D_0$) tend to break by bending owing to the bubble jet induced large impact. Meanwhile, because of the large action range of the impact, these nanowires can be easily broken down. For short ones ($L \leq D_0$), they tend to break by tearing owing to the bubble jet induced tensile force, even when L is slightly longer than D_0, because the jet is gradually expanded. Since the jet is gradually expanded. Therefore, nanowires with such size will not have bending deformation. Apparently, the possibility of the nanowires to be dragged into the bubble jet is quite low as shown in Fig. 1(c), leading to relatively low fracture rate. However, it should be noted that the two fracture mechanisms can take effect on the nanowires with length $L \gg D_0$ simultaneously, still the bending fracture mechanism dominates for the large action range of the impact. Also, the shock wave with same high rate as bubble jet would extend radially. However, the radial propagation of shock wave results in rapid decrease of flow rate when it propagates away from the bubble. Meanwhile, different from the concentration effect of bubble jet on nanowires, the moment of forces on nanowires not far away from the bubble provided by radial propagation of shock wave is very little. Therefore, shock wave could have little effects on nanowires. In addition, the atomic energy induced by the ultrasonic action little effect on the deformation of nanowires, the sonication deformation of nanowires is mainly a mechanics problem.[22]

In order to verify two stages of our fragmentation mechanism, we have selectively chosen two kinds of metal nanowires (Ag and Cu). Due to their good plasticity,[28,29] the force exerted by sonication can be recorded from their deformation. However, the good properties of these metal nanowires can lead to a shortcoming that the deformation is permanent. Hence, two typical nanowires with similar diameters and strength were chosen, whose lengths are distributed in the range of L slightly longer than D_0 and that $L \gg D_0$, respectively. All of our measurements were performed under conditions where the bulk external temperature of the solvent was kept constant at 273 K using a cooling system, to avoid the heating effect which could bring about changes in mechanical properties of metal nanowires after prolonged sonication.

After 2, 4, and 8 min of sonication, the average length of Ag nanowires (diameter 140 nm) was reduced to 12, 11 and 9 μm, as shown by optical microscope (Fig. 3(a)–(d)). Matching with the theoretical expectation, the reduction rate of the average length shows a sharp decrease in the initial 2 min, then gets slower as shown in Fig. 3(e). In addition, a number of bending points are discovered and keep increasing over sonication time as shown in Fig. 3(f). Apparently, the bending deformation of Ag nanowires is still the dominant factor for the average length reduction after the initial bending fracture.

Recently, some fragmentation mechanisms of metal nanomaterials have been revealed from the lattice distortions of metal nanomaterials by *in situ* tests and have aroused

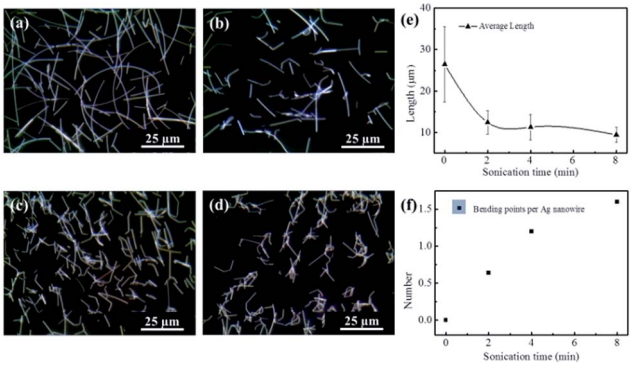

Fig. 3 Optical microscopy images of Ag nanowires. (a) Original morphology of Ag nanowires; (b)–(d) Ag nanowires sonicated after 0, 2, 4, and 8 min; (e) average lengths of Ag nanowires sonicated after 0, 2, 4, and 8 min; (f) statistic bending points per Ag nanowire sonicated after 0, 2, 4, and 8 min.

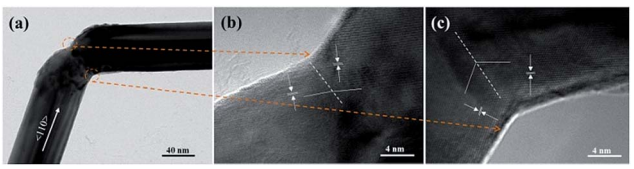

Fig. 4 TEM images of a bending point of Ag nanowire. (a) Morphology of the bending point; (b) and (c) magnified images of the bending point. The white lines marked the crystal orientations, and the white dot lines vertically split the bending point.

great interest.[30,31] The lattice distortions on metal nanowires which always have high orderly lattice arrangement can provide accurate information of the effects of stress on them in nano-scale. In order to determine the exact force-caused bending fracture, the lattice distortions in the bending point are discussed in detail. From TEM results as shown in Fig. 4, twin lattice dislocation (Fig. 4(b)) and coordinated dislocation can be observed (Fig. 4(c)) respectively. These dislocations exhibit a typical impact fragmentation feature based on the classical mechanics of materials, reflecting the remnants affected by bubble jet induced impactions, which is predicted in our model. In addition, selected area electron diffraction (SAED) results (Fig. S1†) show that tiny cracks with lots of dislocations are distributed around the bending points of some nanowires, which reveals a condition that even under relatively low impactions, the bending fracture caused by metal fatigue could happen. Therefore, the effective impact area of bubble jet could have a wider scope than we predicted above.

We now apply our model to the fragmentation of Cu nanowires. Fig. 5 shows the morphology of Cu nanowires sonicated after 0, 60, 80 and 100 min, respectively. During this experiment we adopted a spreading process for sample preparation to separate the aggregated Cu nanowires during sonication,[21] though not completely separated as shown in Fig. 5(a). Initially, no evident changes of Cu nanowires are found and only after prolonged sonication time, notable

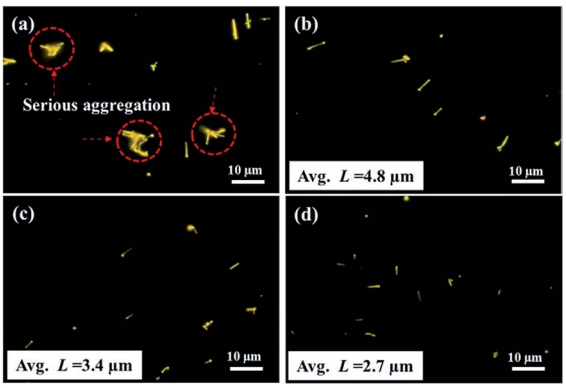

Fig. 5 Optical microscopy images of Cu nanowires. (a) to (d) Morphology of Cu nanowires sonicated after 0, 60, 80 and 100 min.

length reduction of Cu nanowires could be observed (Fig. S2†). Compared with Ag nanowires, a significantly different fracture manner has been observed that most of Cu nanowires keep lineal shapes during sonication process. The observations again are in good agreement with the predictions mentioned above, which plays an active role in determining the length control of nanowires ($L \leq D_0$) without altering linearity.

From above results, our model of ultrasonic fragmentation behaviour of nanowires is further tested. Based on this sonication mechanism, sonication process can realize controllable sizes and morphologies of one-dimensional nanomaterial. As we know, multiple plasmons in metal nanoparticles or nanowires are very sensitive to the particle size and shape, and various works have been undertaken to control their size and shape.[32–35] Recently, Ag nanowires, being applied in the next generation of flexible transparent conductive materials, have attracted considerable attention.[36–38] Since their synthesis and utilization is frequently involved with sonication, here again Ag nanowires are chosen as a case. During the initial sonication period, the absorption of Ag nanowires dispersion solution is enhanced, then gradually reduces by subsequent reaction as shown in Fig. 6. This variation of absorption shows

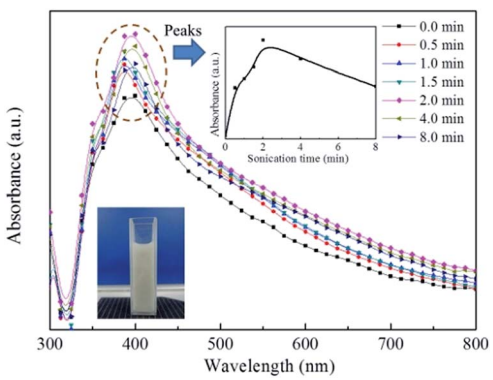

Fig. 6 Absorbance variation of Ag nanowires dispersion solution sonicated for 0, 0.5, 1, 1.5, 2, 4 and 8 min, respectively. Ag nanowires dispersion solution and the value of the peaks are show in the insets.

it is possible to controllably modify the optical properties of Ag nanowires by sonication. The underlying reason is closely related to the fragmentation process (as shown in Fig. 3). Initially, the concentration increase of Ag nanowires upon continuous bending breakage can lead to absorption enhancement for multiple light capture. Thereafter, with the concentration reaching a constant, localized surface plasmon resonance resulting from bends plays a dominant role,[39] directly triggering weakened absorption. Consequently, sonication treatments can provide a cost-effective and eco-friendly modification way for expanding the applications of nanowire materials.

Conclusions

In conclusion, we establish a model to study the influence of sonication-induced bubble jet on the fragmentation mechanisms of solution-dispersed nanowires. This model shows the differences between size-dependent bending fragmentation and tensile fragmentation mechanisms of nanowires. The long nanowires ($L \gg D_0$) with diameter $d < 1$ μm tend to break by bending fragmentation effect of sonication, while short nanowires with diameter $d < 1$ μm (L is slightly longer than D_0 or $L \leq D_0$) broken by tensile effect of sonication, which are corroborated by the experiments and previous studies. In addition, based on the mechanism, sonication treatments provide a novel cost-effective approach for controllable modifications of nanowires. This work provides fundamental understanding of the ultrasonic fragmentation mechanism, and pioneers the extended applications of nanowire materials.

Acknowledgements

This work is supported partially by National High-tech R&D Program of China (863 Program, No. 2015AA034601), National Natural Science Foundation of China (Grant no. 91333122, 61204064, 51202067, 51372082, 51402106 and 11504107), Ph.D. Programs Foundation of Ministry of Education of China (Grant no. 20120036120006, 20130036110012), Par-Eu Scholars Program, and the Fundamental Research Funds for the Central Universities.

Notes and references

1 K. S. Suslick and D. J. Flanningan, *Annu. Rev. Phys. Chem.*, 2008, **59**, 659.
2 F. Hennrich, R. Krupke, K. Arnold, J. A. R. Stutz, S. Lebedkin, T. Koch, T. Schimmel and M. M. Kappes, *J. Phys. Chem. B*, 2007, **111**, 1932.
3 R. Jarretta and R. Crooka, *Mater. Res. Innovations*, 2015, **20**, 86.
4 X. D. Li, Y. Feng, M. C. Li, W. Li, H. Wei and D. D. Song, *Adv. Funct. Mater.*, 2015, **25**, 6858.
5 N. K. Bourne, *Shock Waves*, 2002, **11**, 447.
6 K. S. Suslick and G. J. Price, *Annu. Rev. Mater. Sci.*, 1999, **29**, 295.
7 J. Muller, F. Huaux, N. Moreau, P. Misson, J.-F. Heilier, M. Delos, M. Arras, A. Fonseca, J. B. Nagy and D. Lison, *Toxicol. Appl. Pharmacol.*, 2005, **207**, 221.
8 S. C. B. Mannsfeld, A. Sharei, S. H. Liu, M. E. Roberts, I. McCulloch, M. Heeney and Z. N. Bao, *Adv. Mater.*, 2008, **20**, 4044.
9 G. Schider, J. R. Krenn, A. Hohenau, H. Ditlbacher, A. Leitner and F. R. Aussenegg, *Phys. Rev. B: Condens. Matter Mater. Phys.*, 2003, **68**, 155427.
10 W. H. Wang, Q. Yang, F. R. Fan, H. X. Xu and Z. L. Wang, *Nano Lett.*, 2011, **11**, 1603.
11 C. Park, Z. Ounaies, K. A. Watson, R. E. Crooks, J. Smith Jr, S. E. Lowther, J. W. Connell, E. J. Siochi, J. S. Harrison and T. L. Clair, *Chem. Phys. Lett.*, 2002, **364**, 303.
12 H. G. Flynn, Academic Press, *Physics of acoustic cavitation in liquids*, New York, 1964, ch. 1.
13 F. G. Hammitt, *Natl. Bur. Stand.*, 1974, **394**, 31.
14 V. Belova, D. A. Gorin, D. G. Shchukin and H. Möhwald, *Angew. Chem., Int. Ed.*, 2010, **49**, 7129.
15 V. G. Pola, Y. Li, F. Dogan, E. Secor, M. M. Thackeray and D. P. Abraham, *J. Power Sources*, 2014, **258**, 46.
16 A. D. Wang, L. Jiang, X. W. Li, Y. Liu, X. Z. Dong, L. T. Qu, X. M. Duan and Y. F. Lu, *Adv. Mater.*, 2015, **27**, 6238.
17 E. V. Skorb, D. G. Shchukin, H. Mohwald and D. V. Andreeva, *Nanoscale*, 2010, **2**, 722.
18 Q. H. Cheng, S. Debnath, E. Gregan and H. J. Byrne, *J. Phys. Chem. C*, 2010, **114**, 8821.
19 M. Zheng, A. Jagota, E. D. Semke, B. A. Diner, R. S. Mclean, S. R. Lustig, R. E. Richardson and N. G. Tassi, *Nat. Mater.*, 2003, **2**, 338.
20 D. G. Shchukin, E. Skorb, V. Belova and H. Möhwald, *Adv. Mater.*, 2011, **23**, 1922.
21 K. Kumar, H. G. Duan, R. S. Hegde, S. C. W. Koh, J. N. Wei and J. K. W. Yang, *Nat. Nanotechnol.*, 2012, **7**, 557.
22 Y. Y. Huang, S. V. Ahir and E. M. Terentjev, *Phys. Rev. B: Condens. Matter Mater. Phys.*, 2006, **73**, 125422.
23 Y. Y. Huang, T. P. J. Knowles and E. M. Terentjev, *Adv. Mater.*, 2009, **21**, 3945.
24 J. P. Dear and J. E. Field, *J. Fluid Mech.*, 1988, **361**, 75.
25 C. E. Brennen, *Cavitation and bubble dynamics*, Oxford University Press, New York, 1995, ch. 3.
26 N. Rajaratnam, *Turbulent jets*, Elsevier Scientific Publishing Company, New York, 1976, ch. 1.
27 S. Y. Chang and S. J. Lin, *Scr. Mater.*, 1996, **35**, 225.
28 B. Wu, A. Heidelberg and J. J. Boland, *Nano Lett.*, 2006, **6**, 468.
29 H. S. Park, K. Gall and J. A. Zimmerman, *Phys. Rev. Lett.*, 2005, **95**, 255504.
30 K. Lu, L. Lu and S. Suresh, *Science*, 2009, **324**, 352.
31 J. W. Wang, Z. Zeng, C. R. Weinberger, Z. Zhang, T. Zhu and S. X. Mao, *Nat. Mater.*, 2015, **14**, 594.
32 H. Dai, R. Q. Ding, M. C. Li, J. J. Huang, Y. F. Li and M. Trevor, *Sci. Rep.*, 2014, **4**, 6742.
33 B. N. Khlebtsov and N. G. Khlebtsov, *J. Phys. Chem. C*, 2007, **111**, 11516.
34 H. Dai, M. C. Li, Y. F. Li, H. Yu, F. Bai and X. F. Ren, *Opt. Express*, 2012, **20**, A502.

35 X. L. Zhuo, X. Z. Zhu, Q. Li, Z. Yang and J. F. Wang, *ACS Nano*, 2015, **9**, 7523.
36 D. S. Leem, A. Edwards, M. Faist, J. Nelson, D. D. C. Bradley and J. C. D. Mello, *Adv. Mater.*, 2011, **23**, 4371.
37 E. C. Garnett, W. S. Cai, J. J. Cha, F. Mahmood, S. T. Connor, M. G. Christoforo, Y. Cui, M. D. McGehee and M. L. Brongersma, *Nat. Mater.*, 2012, **11**, 241.
38 Z. B. Yu, Q. W. Zhang, L. Li, Q. Chen, X. F. Niu, J. Liu and Q. B. Pei, *Adv. Mater.*, 2011, **23**, 664.
39 H. Wei, X. R. Tian, D. Pan, L. Chen, Z. L. Jia and H. X. Xu, *Nano Lett.*, 2015, **15**, 560.